

Proposed visible emission line space solar coronagraph

Jagdev Singh*, B. Raghavendra Prasad, P. Venkatakrishnan, K. Sankarasubramanian, Dipankar Banerjee, Raja Bayanna, Shibu Mathew, Jayant Murthy, Prasad Subramaniam, R. Ramesh, S. Kathiravan, S. Nagabhushana, P. K. Mahesh, P. K. Manoharan, Wahab Uddin, S. Sriram, Amit Kumar, N. Srivastava, Koteswara Rao, C. L. Nagendra, P. Chakraborty, K. V. Sriram, R. Venkateswaran, T. Krishnamurthy, P. Sreekumar, K. S. Sarma, Raghava Murthy, K. H. Navalgund, D. R. M. Samudraiah, P. Narayan Babu and Asit Patra

The outer atmosphere of the sun – called the corona – has been observed during total solar eclipse for short periods (typically < 6 min), from as early as the eighteenth century. In the recent past, space-based instruments have permitted us to study the corona uninterruptedly. In spite of these developments, the dynamic corona and its high temperature (1–2 million K) are yet to be fully understood. It is conjectured that their dynamic nature and associated energetic events are possible reasons behind the high temperature. In order to study these in detail, a visible emission line space solar coronagraph is being proposed as a payload under the small-satellite programme of the Indian Space Research Organisation. The satellite is named as Aditya-1 and the scientific objectives of this payload are to study: (i) the existence of intensity oscillations for the study of wave-driven coronal heating; (ii) the dynamics and formation of coronal loops and temperature structure of the coronal features; (iii) the origin, cause and acceleration of coronal mass ejections (CMEs) and other solar active features, and (iv) coronal magnetic field topology and three-dimensional structures of CMEs using polarization information. The uniqueness of this payload compared to previously flown space instruments is as follows: (a) observations in the visible wavelength closer to the disk (down to 1.05 solar radii); (b) high time cadence capability (better than two-images per second), and (c) simultaneous observations of at least two spectral windows all the time and three spectral windows for short durations.

Keywords: Coronal mass ejection, payload, solar coronagraph, spectral window.

THE intensity of the solar corona is million times fainter than that of the photosphere in visible wavelengths. Hence, the solar corona is observed during total solar eclipse (TSE) when the bright photospheric light is blocked by the moon. There has been great progress in coronal studies, from viewing and making sketches of coronal structures to obtaining high-resolution imaging with accurate photometry and spectroscopy during TSE to understand the physical and dynamical characteristics

of the corona. The invention of the coronagraph – a special instrument developed by Lyot using an internal occulter and a Lyot stop to minimize the scattered light within the instrument – has contributed a lot in this direction and has made it possible to observe the corona regularly without the occurrence of a TSE. However, this method is limited to places where scattering from the earth's atmosphere is minimal, which are few around the world, and that too with limited observing periods driven

Jagdev Singh, B. Raghavendra Prasad, Dipankar Banerjee, Jayant Murthy, R. Ramesh, S. Kathiravan, S. Nagabhushana, P. K. Mahesh, S. Sriram and Amit Kumar are in the Indian Institute of Astrophysics, Sarjapur Road, Koramangala, Bangalore 560 034, India; P. Venkatakrishnan, Raja Bayanna, Shibu Mathew and N. Srivastava are in the Udaipur Solar Observatory, Physical Research Laboratory, Badi Road, Udaipur 313 004, India; K. Sankarasubramanian, P. Sreekumar, K. S. Sarma, Raghava Murthy and K. H. Navalgund are in the Space Science Division, Space Astronomy Group, ISRO Satellite Centre, Vimanapura Post, Bangalore 560 017, India; Prasad Subramaniam is in the Indian Institute of Science Education and Research, Sai Trinity Building, Pashan, Pune 411 201, India; P. K. Manoharan is in the Radio Astronomy Centre, Tata Institute of Fundamental Research, Udahgamandalam 643 001, India; Wahab Uddin is in the Aryabhata Research Institute of Observational Sciences, Manora Peak, Naini Tal 263 129, India; Koteswara Rao, C. L. Nagendra, P. Chakraborty, K. V. Sriram, R. Venkateswaran and T. Krishnamurthy are in the Laboratory for Electro-Optics Systems, Peenya, Bangalore 560 058, India; D. R. M. Samudraiah, P. Narayan Babu and Asit Patra are in the Space Application Centre, Jodhpur, Tekra, Ahmedabad 380 015, India. *For correspondence. (e-mail: jsingh@iiap.res.in)

by the local atmospheric conditions. The advancement in space technology has made it possible to study the corona in extreme ultraviolet (EUV) and X-ray wavelength range, which is not feasible from the earth. There has been considerable progress in studying the solar corona over the last several years with space-based instruments on-board Yohkoh, SOHO, TRACE, RHESSI and HINODE. Most of the space-based observations are in EUV and X-ray wavelength range. There are also space missions in visible wavelengths, which are broadband and low resolution ($>4''$ spatial and >1 min temporal) for the study of coronal mass ejections (CMEs) in the outer solar corona ($>2 R_{\odot}$).

It was realized only in 1939 that the solar corona is hotter (1–2 million K) than the photosphere (5700 K)¹. There are theories that invoke the existence of waves and their dissipation in the solar corona. Some authors consider that the existence of large-scale reconnections cause eruptive prominences, flares and CMEs, and some others use the existence of micro/nano flares to explain the heating of the corona. Generally it is agreed that magnetic energy is responsible for the heating of coronal plasma, but the physical processes involved are not yet fully understood.

Apart from the spatially averaged high temperature of the solar corona, there are other dynamic phenomena which are expected to play a part in heating the corona as well as throw energetic particles to the inter-planetary medium and hence directly affect the space weather. CMEs are now recognized to be among the primary drivers of space weather disturbances and related geomagnetic effects. With our increasing dependence on technologies that are vulnerable to space weather transients, it has become crucially important to understand the various components in the overall 'sun–earth transmission line'². The study of CMEs has arguably been the most prominent scientific contribution from modern coronagraphs, including the pioneering LASCO coronagraph aboard the SOHO spacecraft. The advantages of space-borne CME observations over ground-based ones are low levels of scattered light and immunity to variations in sky transparency. The vast extent of scientific results concerning CMEs from space-borne coronagraphs amply validates the utility of space-based CME observations.

A visible emission line space solar coronagraph is proposed keeping in view the available data, and the existing and possible future space experiments. This experiment will yield complementary data in the inner corona with relatively high spatial and temporal resolution. The payload is designed to take images of the solar corona in the red (at 637.4 nm) and green (at 530.3 nm) emission lines simultaneously at a cadence of two images per second with a pixel resolution of 1.4 arcsec, covering the coronal region from 1.05 to 1.50 R_{\odot} . These emission lines are due to highly ionized atoms ([Fe x] and [Fe xiv] respectively)

and hence represent plasma at a temperature of 1.0 and 1.8 million K, respectively. The payload is also designed to take images of the solar corona in continuum radiation around 580 nm, with a pixel resolution of 2.8 arcsec and a field-of-view (FOV) of 3 R_{\odot} for the CME studies. The images obtained in the green line through polarization analysis optics along with the continuum polarization images can also provide the topology of magnetic fields in the solar corona. The continuum polarization images themselves can provide three-dimensional information on CMEs.

In the following sections, the current status of the science goals to be studied with this payload and how the proposed instrument will help generate further information to advance our understanding about the physical and dynamical processes, are discussed in detail. The preliminary optical design of this payload is also discussed.

Proposed science goals

High-frequency intensity oscillations

Several studies^{3–5} emphasize the relevance of high-frequency coronal waves to coronal heating. The existence of waves in the solar corona is likely to create high-frequency intensity, velocity and/or line-width oscillations depending on the nature of the waves. Koutchmy *et al.*⁶ reported velocity oscillations with periods near 300, 80 and 43 s, but found no prominent intensity fluctuations from the measurements of the green-line profiles. Liebenberg and Hoffman⁷ found 300 s oscillations from their Concorde observations of the 1973 eclipse, indicating the heating of the solar corona by acoustic waves, which was soon discarded due to OSO-8 observations.

Singh *et al.*⁸ found intensity oscillations in the 0.02–0.2 Hz range, with amplitudes of 0.2–1.3% during the 1995 eclipse. Cowsik *et al.*⁹ and Singh *et al.*¹⁰ confirmed these detections from the observations during the 1998 and 2006 eclipses (Figure 1) respectively. Phillips *et al.*¹¹ and Williams *et al.*¹² reported successful Charge-Coupled Device (CCD) observations of 6 s oscillations during the 1999 eclipse; but the results were inconclusive for higher frequencies. Pasachoff *et al.*¹³ obtained a series of coronal images using two CCD cameras during the 1999 eclipse, and suggested the presence of enhanced power, particularly in the 0.75–1 Hz range. They concluded that MHD waves remain a viable method of coronal heating. From the spectroscopic observations, Singh *et al.*^{14–18} found that the width of the red line increases with height, whereas that of the green line decreases above the limb. The intermediate temperature emission lines do not show much change in width with height. O'Shea *et al.*¹⁹ reported that the decrease in line width in coronal lines at large heights from the solar limb may not simply be related to the dissipation of wave energy. The existence of waves in the

solar corona is expected to cause an increase in line width with height. The different behaviour of coronal emission lines (CELs) with height imposes certain restrictions on the existing models of coronal heating and suggests a detailed study to understand the nature of waves in the solar corona.

In the proposed experiment, simultaneous high cadence images of the green and red-line corona will be obtained. The images will then be used to detect the spatial and temporal variations in a variety of coronal structures using Fourier and wavelet analysis. These would then be available as inputs for aiding theoretical understanding of wave heating of the corona.

Dynamics of coronal loops

Cooling of post-flare coronal loops: It is generally believed that high-temperature plasma is produced via reconnection during the occurrence of a solar flare. From the observations of the Ca xv line at 569.4 nm (representing plasma at about 4 million K), and green and red lines of a flaring region, Ichimoto *et al.*²⁰ have shown that the high-temperature plasma produced during a flare is diffuse and does not show well-defined coronal loops. These observations were not simultaneous and they could therefore not comment on the cooling of the loops. Similarly, images of the solar corona taken in the EUV lines using EIT instruments on-board SOHO and TRACE are not simultaneous and thus are unable to yield information about the cooling of the coronal loops. Generally, it is postulated that the loops cool by the radiation process. In that case the loops should cool down in a couple of minutes and disappear when observed in high-temperature emission lines, but these loops continue to be visible for long durations.

Temperature structure of coronal loops: The intensity ratio obtained from the emission lines of the same species yields the temperature of the emitting plasma. Guhathakurta *et al.*^{21,22} studied the intensity ratio of green to red line to study the variation of coronal temperature with the solar cycle phase. They have the intensity measurements only near the limb and at certain points in the solar corona and thus could not study the variation of temperature along the coronal loops. Raju and Singh²³ computed the flux of these lines as a function of temperature and density. When they compared this with the observed intensities as a function of height, they found the coronal temperature to be 1.5 million K at the epoch of the 1980 eclipse. Kano and Tsuneta²⁴ found the loop tops to be hotter compared to the footpoints, whereas some of the loops have been found to have cooler loop tops²⁵. The data available are limited to study the circumstances for such type of behaviour of different coronal loops. It is important to know the temperature variation in

coronal loops to make realistic models and also to understand the heating process in the solar corona.

Formation, development and dynamics of coronal loops:

The formation and development of coronal loops is poorly known as available data are of low cadence. It is, therefore, not clear if the plasma in the coronal loops comes from the sun or from the local corona itself. Singh *et al.*²⁶ found the formation of a coronal loop by evaporation using the data obtained with the 10 cm and 25 cm coronagraphs at the Norikura Observatory. Note that these observations were carried out in the green and red emission lines, but not simultaneously. The Transition Region Coronal Explorer (TRACE) has provided data for the solar coronal observations with a spatial resolution of 1 arcsec in the EUV region. These data are used to study the density variations along the loop length, and hence the pressure-scale height and the corresponding temperature^{27,28}. Winebarger *et al.*²⁹ observed that cooling loops are not in hydrostatic equilibrium and could be indicative of the fact that the cooling loops do not have energy balance between heating and cooling, and thus are not likely to be in equilibrium. Evolution of density and pressure-scale heights will provide new information on the thermal evolution of loops.

Apparent flows in active-region loops can be measured using feature-tracking algorithms. Any inhomogeneities in the flow show up as a feature which moves along with the flow. By tracking these inhomogeneities the flow speed can be estimated, as done with TRACE and analysed by Winebarger *et al.*³⁰. More complicated flows like helical or rotational flows are observed in apparently sheared or twisted loops³¹. Bi-directional or counter-streaming flows³² and highly fragmented downflows in catastrophically cooling loops (called coronal rains)³³ are also observed. In addition, if the moving features also possess spatial periodicity, then the motion can be interpreted as waves.

High spatial ($\sim 2''$) and temporal (~ 1 min) resolution observations (similar to Figure 2) of coronal loops in two emission lines will provide data to study the temperature structure of the coronal loops and its dynamics during flares and quiescent phase. The dataset will also answer questions on the formation mechanism of loops as well the reason for cooler or hotter loop tops.

Coronal magnetic field topology

Resonance scattering of the photospheric radiation by atoms in the corona produces scattering polarization which is known as Hanle effect. The mechanism which produces CEL polarization is similar to the Hanle effect, but the resulting polarization signals are different due to different coherency properties between magnetic sub-states. For coronal forbidden lines, the Einstein

A-coefficient is small and hence the atoms are in the ‘effectively strong’ field regime of the Hanle polarization³⁴. In this regime, the linear polarization is insensitive to the magnetic field strength and is either parallel or perpendicular to the plane-of-the-sky (POS) magnetic field direction. Note also that the linear polarization becomes zero at the Van Vleck angle and is well-known as the Van Vleck effect³⁵. Circular polarization will be dependent on the field strength. A classical theory of the CEL polarization for both linear and circular polarization has been derived by Lin and Casini³⁶.

For coronal field strengths, circular polarization measurements require high spectral resolution and higher sensitivity than linear polarization measurements. Moreover, LOS measurements alone will not be useful for knowing the strength of the POS magnetic field. Hence, linear polarization measurement alone have been planned for this mission. The POS magnetic field will be useful in estimating the twist of the magnetic region which is a useful parameter to study and understand eruptions like flares and CMEs in the corona. However, coronal magnetic-field estimates need to be made in order to completely understand the physics of these eruptions, which can be obtained either using NLFF photospheric field extrapolations or through radio measurements at these heights³⁷.

The linear polarization measurements in the continuum wavelengths will provide density diagnostics of the coronal plasma, which when combined with the CEL

measurements will provide valuable data on the global evolution of large-scale coronal structures, in particular, on the magnetic processes leading to a CME. From the continuum polarization to non-polarization brightness, it is also possible to derive the 3D structure of CMEs, which is essential to understand their initiation mechanism (source region) as well as their propagation in the interplanetary medium (and hence for space weather). The first attempts in this direction were made by Poland and Munro³⁸ using polarization measurements obtained with Skylab. This was followed by Moran and Davila³⁹ who used polarimetric measurements obtained by LASCO/SoHO in white light to infer the 3D structure. A similar study was carried out by Dere *et al.*⁴⁰. The triangulation technique used with STEREO images^{41,42} confirms that the 3D estimation using polarimetric technique is indeed valid. Hence, the continuum polarization measurements from *Aditya-1* can provide 3D information of the CMEs, as well as the location of the source regions from it.

CME studies and space weather

There are reasonably good data in the height range spanning approximately 2.5 to around 30 R_{\odot} , and our understanding of CME propagation has been greatly enhanced with these data. However, the crucial inner coronal heights (approximately 1–2 R_{\odot}), where the ill-understood process of CME acceleration takes place, is not covered by these data. The now-defunct C1 coronagraph aboard SOHO yielded data in this range (Figure 3), and there have been some interesting results from them, although its cadence and dynamic range were rather limited. Our understanding of CME initiation and acceleration is thus currently limited to inferences from on-disk data (EUV or

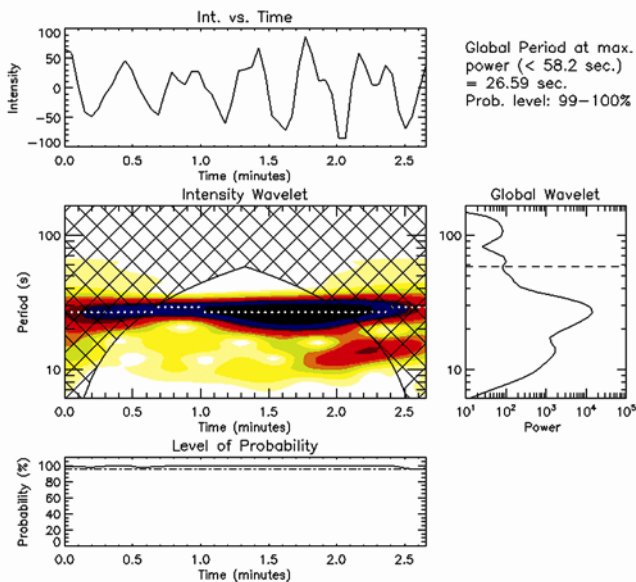


Figure 1. Wavelet analysis for the green-line intensity corresponding to a location in the corona. (Top) Relative intensity (background trend removed). (Middle) Colour-inverted wavelet power spectrum. (Bottom) Variation of probability estimate associated with maximum power in the wavelet power spectrum (marked with dashed lines). (Middle, right) Global (averaged over time) wavelet power spectrum. The period measured from the maximum power from the global wavelet together with probability estimate, is printed¹⁰.

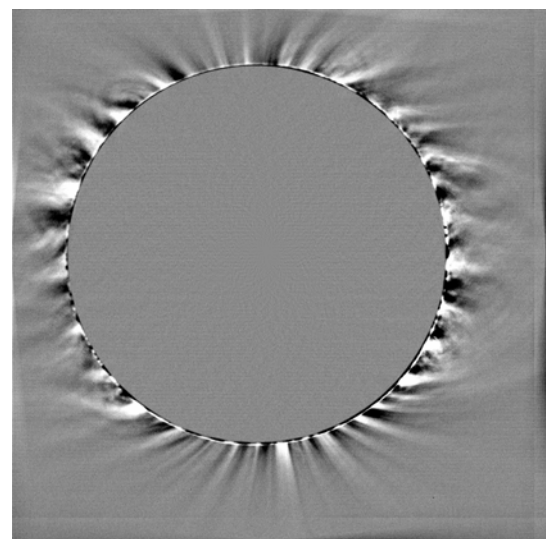


Figure 2. Processed image of the solar corona taken with green filter during the total solar eclipse of 22 July 2009.

soft X-ray) and to questionable extrapolations of CME height–time profiles from coronagraph observations upwards of approximately $2 R_{\odot}$.

In general, the process of CME initiation involves a wide range of spatial and temporal scales. The spatial scales range from a fraction of a typical active region size to nearly a solar radius. The temporal scales range from typical Alfvén timescales (a few to tens of seconds), to several minutes. These features pose significant challenges for theoretical simulations of CME initiation, which is partly why they rely on highly simplified and idealized configurations. Observations of CME initiation have also been severely handicapped for similar reasons.

The proposed coronagraph has the potential to effectively address several CME initiation questions:

- Flux rope-like structures are known to play an important part in the overall development of CMEs^{43,44}. But do coronal cavities/flux ropes exist prior to eruption, as predicted by Low⁴⁵.

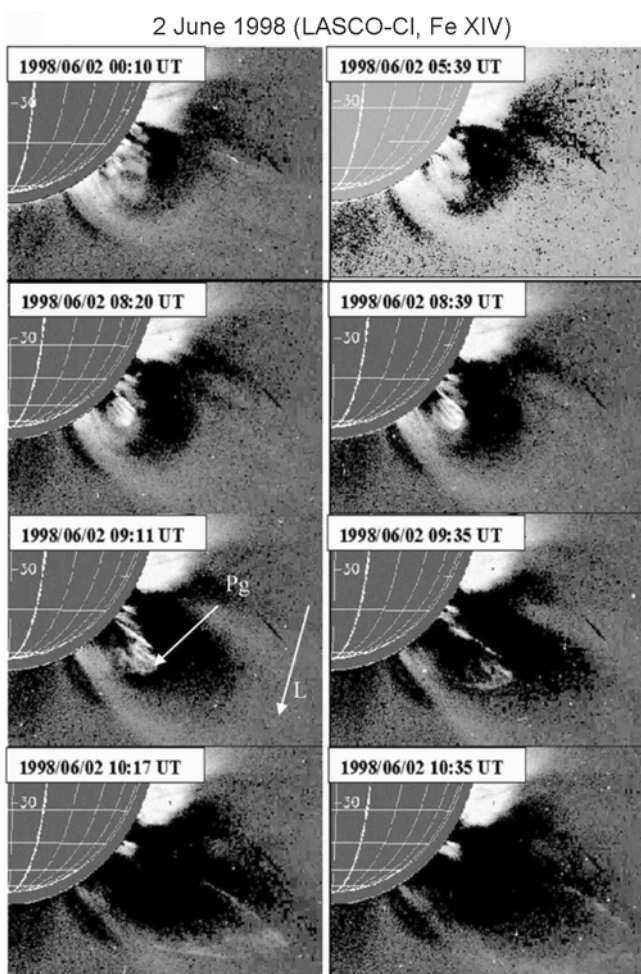


Figure 3. Temporal evolution of coronal mass ejection (CME) as seen in the inner corona by LASCO-C1 on 2 June 1998. The CME shows a dense knot (P_g) embedded within a large overlying loop (L) (Adapted from Srivastava *et al.*⁵⁴).

- The popular breakout model of CMEs⁴⁶ suggests that flux ropes are formed as a byproduct of the reconnection processes leading to the initiation of CMEs, and that they need not be pre-existing entities. Most of the current observational evidence for flux ropes comes from observations above $\sim 2 R_{\odot}$, and the situation closer to the solar limb is far from clear.
- Where does the primary ‘trigger’ reconnection responsible for CME initiation take place: above the erupting flux system, as predicted by the breakout model^{46,47} or below it, as predicted by the ‘tether-cutting’ model? Whereas it is difficult to reliably detect signatures of reconnection, high cadence observations of the movement of coronal loops leading to CME initiation can provide good answers.
- As a corollary, is magnetic complexity an absolute necessity for CME initiation, as required by the breakout model?

Space weather studies are going to be one of the major thrust areas for the international community during the next decade. With the increase in the number of satellites as well as manned operations in space, it is necessary to understand the space weather conditions. The Gauribidanur radioheliograph provides useful information regarding the on-disk development and early stages of CME propagation^{48–50}. The Ooty Radio telescope provides useful information on the propagation characteristics of CMEs beyond around 40 solar radii, the region currently inaccessible to space-borne coronagraphs^{51,52}.

Data from these ground-based instruments, other international space missions (which cover regions from $3 R_{\odot}$ to several R_{\odot}) and from the proposed space coronagraph can thus form a comprehensive basis for studying the entire range of CME-related space weather effects from the sun to the near-earth environment, and positively improve the predictability of space weather events.

Optical design of the proposed coronagraph

A coronagraph is a specialized telescope to observe the corona and can be classified as internal or external depending on the occultation. Internally occulted coronagraphs help in observing the corona close to the solar limb, provided the scattered light is controlled using high-quality optical components. In the case of externally occulted coronagraphs, the requirement on the quality of optical components is not stringent. However, vignetting of inner coronal light, boom length and⁸ are the basic limitations.

An on-axis system with a lens is the simplest approach for a compact and yet provides minimum aberration. However, it is ruled out due to the following reasons: (1) inherent nature of glass to become black when exposed to high-energy radiation in space, absorption of thermal infra-red radiations hence degradation in the image quality,

(2) scatter due to the non-uniformities within the material and (3) chromatic aberration. The use of a mirror avoids any multiple reflections and chromatic aberrations as in the case of lenses, and an off-axis design would reduce the scattered light resulting from the spiders of the secondary mirror⁵³.

Optical design details

An entrance aperture (EA) of 150 mm at a distance of 1.5 m from the objective mirror allows sunlight and coronal light up to $\pm 3.0 R_{\odot}$ to fall on the off-axis parabolic (OAP) mirror (Figure 4). The OAP primary mirror of 1.3 m focal length and clear aperture of 20 cm are used to form primary image at its focal plane and away from the entrance aperture by a distance of 5 cm. A mirror (M2) having a central hole equal to $1.05 R_{\odot}$ placed at the prime focus allows the disk light to pass and reflects the rays corresponding to $\pm 1.05 R_{\odot}$ – $\pm 3.0 R_{\odot}$ towards a collimating lens, which then images the entrance aperture at a distance of 20 mm from its last surface. This is achieved in combination with the curved mirror M2. The sun disk is directed back to the space – through a hole – by a concave mirror M3 that limits the divergence. Lyot stop is placed at the pupil plane to remove the diffraction ring due to the edges of the entrance aperture. The collimated beam is then imaged according to the required plate scale using an off-axis mirror M4 along with the lenses. The dichroic filter DBS-1 splits the beam in two parts; the beam with wavelength greater than 590 nm is reflected to one of the CCD camera using a flat mirror FM1. A narrow band filter with 0.3 nm pass band (effective pass 0.45 nm due to converging beam) centred around 637.4 nm and a lens form an image of the solar corona on the CCD with a spatial resolution of 1.4 arcsec per pixel. The transmitted portion of the beam through DBS-1 passes through a polarization filter wheel that has three polarizing

filters, one clear glass as focal length compensator and an opaque slot to obtain dark images. Then the beam falls on another dichroic filter, DBS-2, that reflects beams with wavelength below 570 nm and transmits those with wavelength in the range 570–590 nm. The reflected beam is used to form an image of the solar corona in the green line with the help of a folding mirror M2, narrow band filter (0.3 nm around the green line), lens and a CCD camera. A triplet lens in the path of the transmitted beam forms an image of the solar corona in the continuum with pixel resolution of 2.8 arcsec. The detailed specifications of each optical component have been worked out for the diffraction limited imaging.

Detectors

The detector planned for this payload is the CCD. The payload requires three different detector modules and at least two of them will be operated simultaneously. One of the scientific goals (intensity oscillations) of the payload require a detector with fast readout rate of four frames per second. The FOV requirement from the science goal necessitates CCDs with a $2\text{ k} \times 2\text{ k}$ chip format and a pixel size of about $13\ \mu\text{m}$. The full-well capacity of $>100,000$ electrons will provide the required dynamic range and photometric accuracy.

There will be four basic modes of payload operation: (i) fast cadence with low spatial resolution and limited FOV; (ii) medium cadence with high spatial resolution and limited FOV; (iii) low cadence with medium spatial resolution and large FOV; and (iv) polarimetric observations keeping in view the different scientific objectives. In a single observing day, the coronagraph will be operated in one or multiple observing modes. In the case of polarization observations, to bring up the signal-to-noise ratio about 25 frames will be added after doing the off-line shift correction.

Satellite requirements

The stability and pointing accuracy of the coronagraph drives the satellite requirements. This is because any small offset in the pointing will offset the image at M2 and hence the possibility of more scattered light into the imaging system as well as the large heat load onto M2, which may reduce the life expectancy of the payload.

The requirements of the space platform and the data rate are specified in Table 1. The pointing accuracy is calculated in such a way that when the image is acquired, the pointing needs to be accurate to 30 arcsec or better. In the interest of stability, it is assumed that there are no exposures above 2 s during the high-resolution observations. The magnitude of the jitter is calculated so that the total image shift does not exceed one pixel.

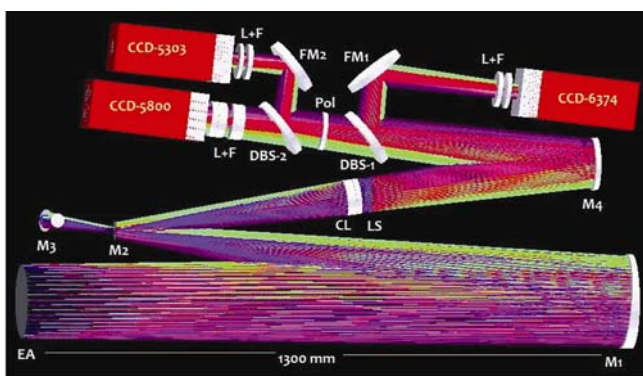


Figure 4. Schematic of the payload. EA, Entrance aperture; M1, Off-axis parabolic mirror; M2, Secondary mirror with a hole; M3, Mirror to remove the disk light; CL, Collimating lens; LS, Lyot stop; M4, Imaging parabola; DBS-1 and DBS-2, Dichroic beam splitters; FM, Folding mirrors; L + F, Combination of lens and filter.

Table 1. Spacecraft specifications required for the space solar coronagraph

Parameter	Requirement
Pointing	Sun
Stabilization	Three-axis body stabilization
Pointing accuracy	30 arcsec (0.0083 degrees) at 3- σ level
Stability	0.25 arcsec per s (7×10^{-5} degrees/s)
Jitter	0.5 arcsec
Weight	130 kg
Orbit	Sun-synchronous polar orbit
Power	130 W raw power
Payload data rate	32 Mbps
Telemetry	105 Mbps
On-board storage	64 Gbits

The on-board storage is estimated for the optimum use of the four different basic modes of operation. These modes will be the basis to carry out the science goals. The standard parameters used in these calculations are: pixel size – $1.4'' \times 1.4''$; number of pixels – $2K \times 2K$, and maximum frame rate of the camera – 4 Hz. It is expected that about 64 Gbits of data will be obtained each day and hence a data storage capability of at least 64 Gbits is required.

- Edlen, B., Die deutung der emissionslinien im spektrum der sonnenkorona. Mit 6 abbildungen. *Z. Astrophys.*, 1943, **22**, 30–64.
- Dryer, M., Interplanetary studies: Propagation of disturbances between the sun and the magnetosphere. *Space Sci. Rev.*, 1994, **67**, 363–419.
- Stein, R. F. and Leibacher, J., Waves in the solar atmosphere. *Annu. Rev. Astron. Astrophys.*, 1974, **12**, 407–435.
- Ionson, J. A., Resonant absorption of Alfvénic surface waves and the heating of solar coronal loops. *ApJ*, 1978, **226**, 650–673.
- Hollweg, J., Alfvén waves in the solar atmosphere. II—Open and closed magnetic flux tubes. *Sol. Phys.*, 1981, **70**, 25–66.
- Koutchmy, S., Zhugzhda, I. D. and Locans, V., Short period coronal oscillations – observation and interpretation. *Astron. Astrophys.*, 1983, **120**, 185–191.
- Liebenberg, D. H. and Hoffman, M. M., Temporal observations of the Fe I 5303 emission line profile during the 74 minute totality from the concorde SST at the 30 June 1973 total solar eclipse: preliminary intensity variations above an active region. IAU Symposium, 1974, vol. 57, pp. 485–487.
- Singh, J. *et al.*, Detection of short-period coronal oscillations during the total solar eclipse of 24 October 1995. *Sol. Phys.*, 1997, **170**, 235–252.
- Cowsik, R., Singh, J., Saxena, A. K., Srinivasan, R. and Raveendran, A. V., Short-period intensity oscillations in the solar corona observed during the total solar eclipse of 26 February 1998. *Sol. Phys.*, 1999, **188**, 89–98.
- Singh, J. *et al.*, Intensity oscillation in the corona as observed during the total solar eclipse of 29 March 2006. *Sol. Phys.*, 2009, **260**, 125–134.
- Phillips, K. J. H. *et al.*, SECIS: The solar eclipse coronal eclipse imaging system. *Sol. Phys.*, 2000, **193**, 259–271.
- Williams, D. R. *et al.*, High-frequency oscillations in a solar active region coronal loop. *MNRAS*, 2001, **326**, 428–436.
- Pasachoff, J. M., Babcock, B. A., Russell, K. D. and Seaton, D. B., Short-period waves that heat the corona detected at the 1999 eclipse. *Sol. Phys.*, 2002, **207**, 241–257.
- Singh, J., Ichimoto, K., Imai, H., Sakurai, T. and Takeda, A., Spectroscopic studies of the solar corona I. spatial variations in line parameters of green and red coronal lines. *PASJ*, 1999, **51**, 269–276.
- Singh, J., Sakurai, T., Ichimoto, K., Suematsu, Y. and Takeda, A., Spectroscopic studies of the solar corona II. Properties of green and red emission lines in open and closed coronal structures. *PASJ*, 2002, **54**, 793–806.
- Singh, J., Ichimoto, K., Sakurai, T. and Muneer, S., Spectroscopic studies of the solar corona. IV. Physical properties of coronal structure. *ApJ*, 2003, **585**, 516–523.
- Singh, J., Sakurai, T., Ichimoto, K. and Watanabe, T., Complex variations in the line-intensity ratio of coronal emission lines with height above the limb. *ApJL*, 2004, **617**, L81–L84.
- Singh, J., Sakurai, T. and Ichimoto, K., Do the line widths of coronal emission lines increase with height above the limb?. *ApJ*, 2006, **639**, 475–483.
- O’Shea, E., Banerjee, D. and Doyle, J. G., On the widths and ratios of Mg X 609.79 and 624.94 Å lines in polar off-limb regions. *Astron. Astrophys.*, 2005, **436**, L35–L38.
- Ichimoto, K., Hara, H., Takeda, A., Kumagai, K., Sakurai, T., Shimizu, T. and Hudson, H. S., Coordinated observation of the solar corona using the Norikura coronagraph and the YOHKOH soft X-ray telescope. *ApJ*, 1995, **445**, 978–981.
- Guhathakurta, M., Fisher, R. R. and Altrrock, R. C., Large-scale coronal temperature and density distributions, 1984–1992. *ApJL*, 1993, **414**, L145–L148.
- Guhathakurta, M., Fisher, R. and Strong, K., Temperature structure of the high-latitude corona. *ApJL*, 1996, **471**, L69–L71.
- Raju, P. K. and Singh, J., Comparison of computed fluxes for Fe X and Fe XIV lines with observed values at 1980 eclipse. *Sol. Phys.*, 1987, **110**, 271–280.
- Kano, R. and Tsuneta, S., Temperature distributions and energy scaling law of solar coronal loops obtained with YOHKOH. *PASJ*, 1996, **48**, 535–543.
- Singh, J., Sakurai, T. and Ichimoto, K., Detection of coronal loop-tops in coronal structure. *Asian J. Phys.*, 2004, **13**, 245–250.
- Singh, J., Sakurai, T., Ichimoto, K., Suzuki, I. and Hagino, M., Spectroscopic studies of solar corona VII. Formation of a coronal loop by evaporation. *Sol. Phys.*, 2005, **226**, 201–221.
- Ashwanden, M. J., Alexander, D., Hurlburt, N., Newmark, J. S., Neupert, W. M., Klimchuk, J. A. and Gary, G. A., Three-dimensional stereoscopic analysis of solar active region loops. II. SOHO/EIT Observations at temperatures of 1.5–2.5 MK. *ApJ*, 2000, **531**, 1129–1149.
- Singh, J., Sakurai, T., Ichimoto, K. and Takeda, A., Spectroscopic studies of the solar corona III. Density diagnostics using the infrared lines of Fe XIII. *PASJ*, 2002, **54**, 807–816.
- Winebarger, A. R., DeLuca, E. E. and Golub, L., Evolving active region loops observed with the transition region and coronal explorer. I. Observations. *ApJ*, 2001, **553**, L81–L84.
- Winebarger, A. R., Warren, H. P. and Seaton, D. B., Apparent flows above an active region observed with the transition region and coronal explorer. *ApJ*, 2003, **593**, 1164–1173.
- Chae, J., Wang, H., Qiu, J., Goode, P. R. and Wilhelm, K., Active region loops observed with SUMER on board the SOHO. *ApJ*, 2000, **533**, 535–545.
- Qiu, J., Wang, H., Chae, J. and Goode, P. R., Counter-streaming mass flow and transient brightening in active region loops. *Sol. Phys.*, 1999, **190**, 153–165.
- Schrijver, C. J., Catastrophic cooling and high-speed downflow in quiescent solar coronal loops observed with TRACE. *Sol. Phys.*, 2001, **198**, 325–345.
- House, L. L., Coronal emission-line polarization from the statistical equilibrium of magnetic sublevels. I—Fe XIII. *ApJ*, 1977, **214**, 632–652.
- House, L. L., The theory of the polarization of coronal forbidden lines. *PASP*, 1974, **86**, 490–499.

GENERAL ARTICLES

36. Lin, H. and Casini, R., A classical theory of coronal emission line polarization. *ApJ.*, 2000, **542**, 528–534.
37. Ramesh, R., Kathiravan, C. and Sastry, Ch. V., Metric radio observations of the evolution of a ‘Halo’ coronal mass ejection close to the sun. *ApJ.*, 2003, **591**, L163–L166.
38. Poland, A. I. and Munro, R. H., Interpretation of broad-band polarimetry of solar coronal transients – importance of H-alpha emission. *ApJ.*, 1976, **209**, 927–934.
39. Moran, T. G. and Davilla, J. M., Three-dimensional polarimetric imaging of coronal mass ejections. *Science*, 2004, **305**, 66–71.
40. Dere, K. P., Wang, D. and Howard, R., Three-dimensional structure of coronal mass ejections from LASCO polarization measurements. *ApJ.*, 2005, **620**, L119–L122.
41. Mierla, M. *et al.*, A quick method for estimating the propagation direction of coronal mass ejections using STEREO-COR1 images. *Sol. Phys.*, 2008, **252**, 385–396.
42. Srivastava, N., Inhester, B., Mierla, M. and Podlipnik, B., 3D Reconstruction of the leading edge of the 20 May 2007 partial halo CME. *Sol. Phys.*, 2009, **259**, 213–225.
43. Chen, J. *et al.*, Evidence of an erupting magnetic flux rope: LASCO Coronal mass ejection of 13 April 1997. *ApJL*, 1997, **490**, L191–L194.
44. Dere, K. P., Brueckner, G. E., Howard, R. A., Michels, D. J. and Delaboudiniere, J. P., LASCO and EIT observations of helical structure in coronal mass ejections. *ApJ.*, 1999, **516**, 465–474.
45. Low, B. C., Solar activity and the corona. *Sol. Phys.*, 1996, **167**, 217–265.
46. Antiochos, S. K., DeVore, C. R. and Klimchuk, J. A., A model for solar coronal mass ejections. *ApJ.*, 1999, **510**, 485–493.
47. Lynch, B. J., Antiochos, S. K., MacNeice, P. J., Zurbuchen, T. H. and Fisk, L. A., Observable properties of the breakout model for coronal mass ejections. *ApJ*, 2004, **617**, 589–599.
48. Kathiravan, C., Ramesh, R. and Subramanian, K. R., Metric radio observations and ray-tracing analysis of the onset phase of a solar eruptive event. *ApJ.*, 2002, **567**, L93–L95.
49. Ramesh, R., Kathiravan, C. and Sastry, Ch. V., Estimation of magnetic field in the solar coronal streamers through low frequency radio observations. *ApJ.*, 2010, **711**, 1029–1032.
50. Kathiravan, C. and Ramesh, R., Identification of the source region of a ‘Halo’ coronal mass ejection using meter-wavelength radio data. *ApJ.*, 2005, **627**, L77–L80.
51. Manoharan, P. K. *et al.*, Coronal mass ejection of 14 July 2000 flare event: imaging from near-sun to earth environment. *ApJ.*, 2001, **559**, 1180–1189.
52. Manoharan, P. K., Evolution of coronal mass ejections in the inner heliosphere: a study using white-light and scintillation images. *Sol. Phys.*, 2006, **235**, 345–368.
53. Kuhn, J. and Hawley, S. L., Some astronomical performance advantages of off-axis telescopes. *PASP*, 1999, **111**, 601–620.
54. Srivastava, N., Schwenn, R. and Stenborg, G., In Proceedings of the 8th SOHO Workshop: Plasma Dynamics and Diagnostics in the Solar Transition Region and Corona, ESA-SP 446, 621, 1999.

ACKNOWLEDGEMENTS. J.S. thanks Prof. G. Srinivasan for discussions on various aspects of the science goals, and about solar physics from space. We thank Profs U. R. Rao, S. S. Hasan, S. M. Chitre, S. Ananthakrishnan, T. K. Alex, and Kiran Kumar for their support, interest and valuable suggestions at various stages of this project.

Received 12 October 2010; accepted 9 November 2010